

# ALMA observations of Titan's atmospheric chemistry and seasonal variation

M. A. Cordiner<sup>1,2</sup>, J. C. Lai<sup>1,3</sup>, N. A. Teanby<sup>4</sup>, C. A. Nixon<sup>1</sup>,  
M. Y. Palmer<sup>1,2</sup>, S. B. Charnley<sup>1</sup>, A. E. Thelen<sup>5</sup>, E. M. Molter<sup>6</sup>,  
Z. Kisiel<sup>7</sup>, V. Vuitton<sup>8</sup>, P. G. J. Irwin<sup>9</sup> and M. J. Mumma<sup>1</sup>

<sup>1</sup>NASA Goddard Space Flight Center, 8800 Greenbelt Road, Greenbelt, MD 20771, USA  
email: martin.cordiner@nasa.gov

<sup>2</sup>Department of Physics, Catholic University of America, Washington, DC 20064, USA

<sup>3</sup>McMaster University, Hamilton, Ontario, Canada

<sup>4</sup>School of Earth Sciences, University of Bristol, Wills Memorial Building, Queens Road, Bristol, UK

<sup>5</sup>New Mexico State University, 1780 E University Ave, Las Cruces, NM 88003, USA

<sup>6</sup>Astronomy Department, University of California, Berkeley, CA 94720, USA

<sup>7</sup>Institute of Physics, Polish Academy of Sciences, Al. Lotnikow 32/46, 02-668 Warszawa, Poland

<sup>8</sup>Université Grenoble Alpes, CNRS, IPAG, F-38000 Grenoble, France

<sup>9</sup>Clarendon Laboratory, University of Oxford, Parks Road, Oxford, UK

**Abstract.** Results are presented from our ongoing studies of Titan using ALMA during the period 2012–2015, including a confirmation of the previous detection of vinyl cyanide ( $C_2H_3CN$ ), as well as the first spatial map for this species on Titan. Simultaneous mapping of  $HC_3N$ ,  $CH_3CN$  and  $C_2H_5CN$  reveal characteristic abundance patterns for each species that provide insight into their individual photochemical lifetimes, and help inform our understanding of Titan's unique, time-variable atmospheric chemistry and global circulation. A time-sequence of  $HC_3N$  maps covering 38 months reveals a dramatic change in the distribution of this gas consistent with high-altitude photochemical production followed by advection towards the southern (winter) pole, combined with rapid loss in the north after Titan's 2009 seasonal equinox. The 2015  $C_2H_3CN$  and  $C_2H_5CN$  maps show abundance peaks in Titan's southern hemisphere, similar to those observed for the short-lived  $HC_3N$  molecule. The longer-lived  $CH_3CN$ , on the other hand, remains more concentrated in the north.

**Keywords.** Planets and satellites: individual (Titan), line: identification, techniques: interferometric, techniques: spectroscopic, astrochemistry, astrobiology

---

## 1. Introduction

Titan, Saturn's largest moon, has a carbon and nitrogen-rich atmosphere that hosts a complex photochemistry, resulting in the synthesis of a broad array of organic compounds including hydrocarbons, nitrogen-bearing and some oxygen-bearing species (see the review by Bézard *et al.* 2014). By virtue of their large dipole moments, several of Titan's nitriles possess strong rotational transitions in the wavelength range accessible to the Atacama Large Millimeter/submillimeter Array (ALMA). As a result of short photochemical lifetimes (on the order of a few years or less — see Wilson & Atreya 2004; Loison *et al.* 2015), some of these nitrile molecules can be used to probe the seasonally-variable chemistry and dynamics in Titan's upper atmosphere (e.g. Teanby *et al.* 2012; Cordiner *et al.* 2014; Vinatier *et al.* 2015). Understanding the complex

chemistry at play in Titan's atmosphere is a work in progress, and several important problems remain unsolved, such as the origin and composition of the haze particles that envelop Titan, the source of the large negative ions found in the ionosphere, and the long-term behaviour of Titan's climate (Hörst 2017). The advent of ALMA provides a powerful new tool for the study of Titan's atmospheric composition and dynamics. With the end of the Cassini mission in September 2017, there is a strong need for continued, detailed molecular mapping to help test and refine atmospheric chemical/dynamical models for application to Titan and other carbon-rich planetary atmospheres. This will lead to improvements in our understanding of the possible chemical processes occurring on the early Earth, as well as other primitive bodies in our own Solar System and beyond.

The distribution of HC<sub>3</sub>N has previously been studied by Cassini through its infrared (vibrational) emission, but CH<sub>3</sub>CN, C<sub>2</sub>H<sub>3</sub>CN and C<sub>2</sub>H<sub>5</sub>CN have relatively weak IR bands, and have so far only been detected at radio/sub-mm wavelengths. Mapping all these species is now possible with ALMA, and each one provides a unique probe of dynamics and chemistry due to its individual production altitude and photochemical lifetime.

Vinyl cyanide (or acrylonitrile; C<sub>2</sub>H<sub>3</sub>CN), is currently of particular interest due to the work of Stevenson *et al.* (2015), who showed, through theoretical liquid-phase calculations, that this molecule may form thermodynamically stable membranes (known as azotosomes) in liquid methane at the surface temperature of Titan (approximately 94 K). Given that Titan possesses seas of liquid hydrocarbon, vinyl cyanide could be a strong candidate for forming membranes of potential astrobiological importance. Although the presence of C<sub>2</sub>H<sub>3</sub>CN on Titan was previously inferred from mass-spectrometric measurements of its protonated form and (neutral) dissociation fragments (Vuitton *et al.* 2007; Cui *et al.* 2009), the first spectroscopic detection was made only recently by Palmer *et al.* (2017), who reported observations of three mm-wave emission lines in ALMA Band 6. Here we report the detection and mapping of three additional lines of C<sub>2</sub>H<sub>3</sub>CN in Band 7, as well as data on C<sub>2</sub>H<sub>5</sub>CN, CH<sub>3</sub>CN and HC<sub>3</sub>N. Further details of this work are given by Lai *et al.* (2017).

## 2. Observations

The observations presented here come from short (2-3 min) integrations of Titan, obtained for the routine calibration of the ALMA flux scale. Raw interferometric data were obtained from the ALMA Science Archive covering five epochs in the range 2012-07-04 to 2015-08-29. Observed frequencies were in the range 221-349 GHz, with a spectral resolution of 976 kHz. Data were calibrated and processed as described by Cordiner *et al.* (2015). To produce spectral line maps, Titan's continuum was subtracted from the visibility amplitudes before imaging. The point-spread function was deconvolved using the Högbom algorithm, with natural visibility weighting and a threshold flux level of twice the RMS noise in each image. The resulting spatial resolution (FWHM of the Gaussian restoring beam) ranged from  $0.48 \times 0.53''$  to  $0.62'' \times 1.22''$ . For comparison, the angular diameter of Titan's surface was  $0.66''$  to  $0.78''$  on the sky.

## 3. Results

An example spatially integrated spectrum (from 2015-04-29) is shown in Fig. 1, with multiple lines of C<sub>2</sub>H<sub>3</sub>CN, C<sub>2</sub>H<sub>5</sub>CN, CH<sub>3</sub>CN, and vibrationally excited HC<sub>3</sub>N identified and labeled. In addition, two lines of C<sub>3</sub>H<sub>8</sub> (propane) were tentatively detected, as well as two unidentified (U) lines at 347635 MHz and 347719 MHz. For further details of

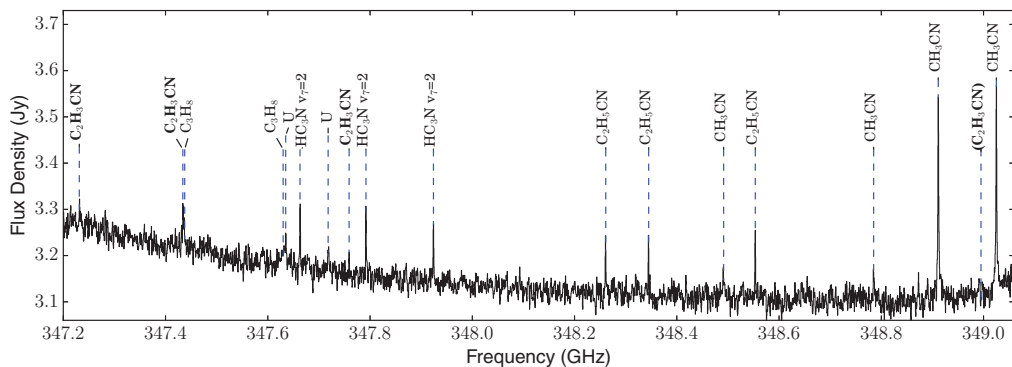


**Figure 1.** ALMA Band 7 spectrum of Titan observed 2015-04-29. Prominent emission lines are assigned by species; bold typeface highlights the  $C_2H_3CN$  emission features. The upwards slope towards lower frequencies is due to the pressure-broadened CO ( $J = 3 - 2$ ) line wing.

the line assignments and radiative transfer modeling see Lai *et al.* (2017). The spatial distribution of flux from each species is shown in the contour maps in Fig. 2, in which the intensity is indicated with an orange color scale and the black contours correspond to increments of  $n\sigma$  (where  $\sigma$  is the RMS noise in each map and  $n$  is a constant factor). The spatial scale is in sky-projected distances with respect to Titan's centre.

The three new  $C_2H_3CN$  emission lines detected improve the confidence level of our previous detection at lower frequency (Palmer *et al.* 2017). They also allow us to map the spatial distribution of this molecule for the first time. Our  $C_2H_3CN$  map (Figure 2; top left) shows a flux peak (at  $5\sigma$  confidence) in Titan's southern hemisphere, consistent with enrichment of this gas over the south polar region. A similar, southerly enrichment is also evident for  $HC_3N$  and  $C_2H_5CN$ . Polar enrichments have previously been observed for a number of hydrocarbons and nitriles by Cassini and ALMA (Teanby *et al.* 2013; Cordiner *et al.* 2015; Vinatier *et al.* 2015). Titan's seasonal cycle is governed by the 29.5 yr orbital period of Saturn. It is theorized that as Titan transitions out of northern winter towards the summer solstice, the main atmospheric circulation cell, responsible for the redistribution of photochemical products from mid-latitudes towards the poles, should reverse its direction (e.g. Teanby *et al.* 2012). During the progression from the 2009 equinox to the southern winter solstice in 2017, the abundances of high-altitude photochemical products are thus expected to begin increasing in the southern polar region, while reactive species concentrated in the north would begin to be destroyed at a rate in accordance with the photochemical lifetime of each molecule.

The southern enhancement in  $C_2H_3CN$  abundance (about a factor of 3 stronger than in the north) is similar to that of  $HC_3N$  at this epoch, whereas the enhancement factor for  $C_2H_5CN$  is somewhat less (about a factor of 1.5), implying a shallower vertical gradient and a longer photochemical lifetime for  $C_2H_5CN$  compared to  $HC_3N$  and  $C_2H_3CN$ . Furthermore, we see a striking difference in the  $HC_3N$  distribution compared with the 2012 observations presented by Cordiner *et al.* (2015) — the  $HC_3N$  peak just three Earth years earlier was firmly in the north, so our ALMA data demonstrate rapid temporal variability of Titan's atmosphere. A factor of possible relevance is the difference in energy between the ground vibrational state transition ( $v = 0$ ,  $E_u = 150$  K) observed by Cordiner *et al.* (2015) and the excited-state ( $v = 2$ ,  $E_u = 970$  K) transition shown in Figure 2. We therefore need to consider the possibility that the previous  $HC_3N$  observation is more sensitive to colder gas, at lower altitudes than that probed by the vibrationally-excited  $HC_3N$  lines. To perform a more robust study of  $HC_3N$  temporal evolution, we need to

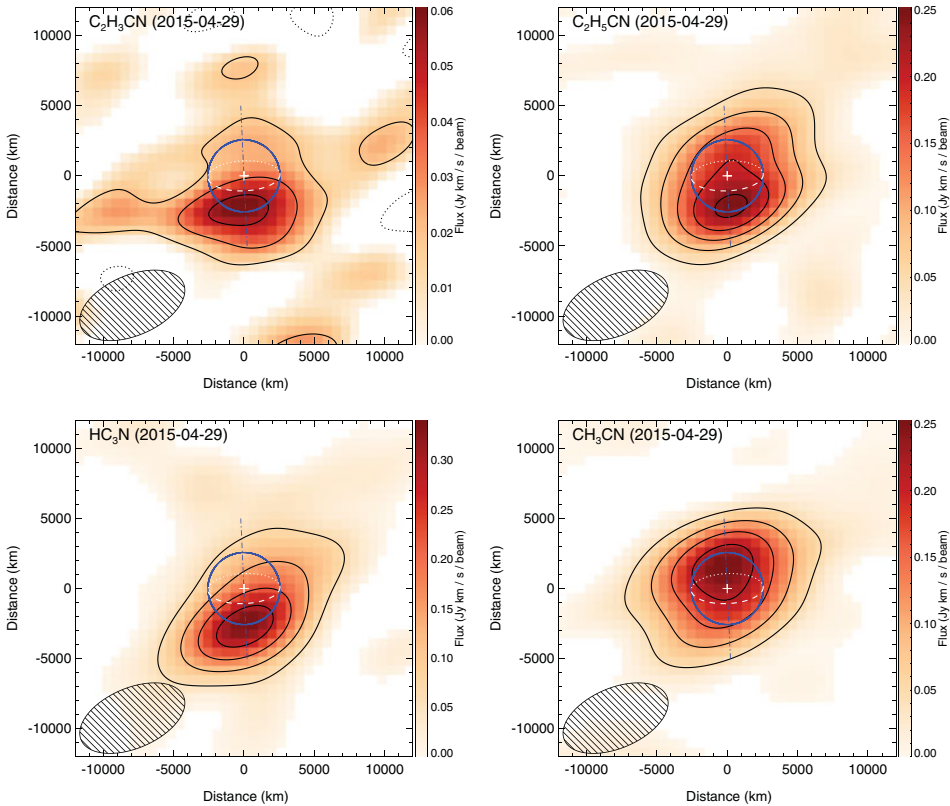
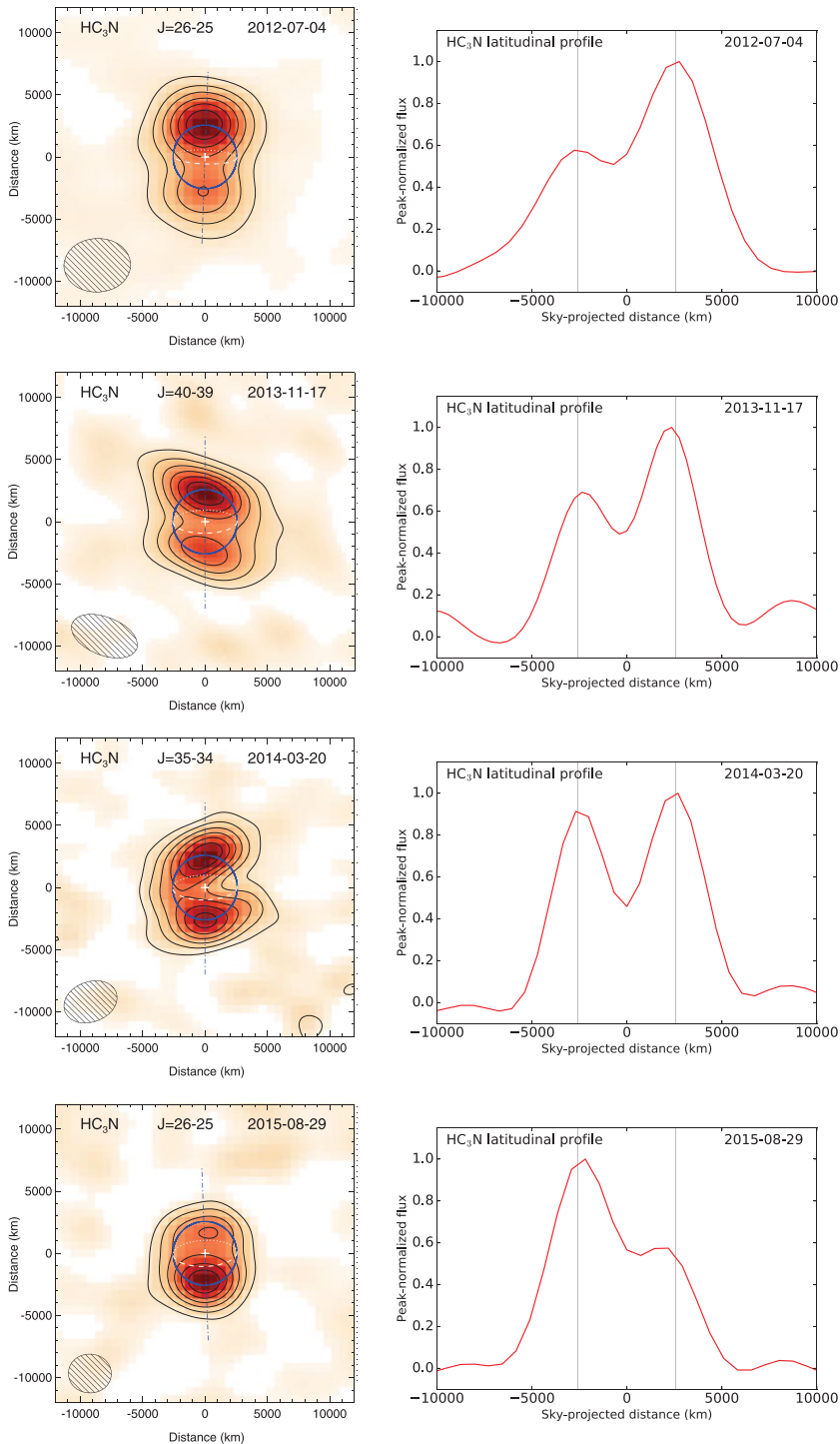


**Figure 2.** Flux contour maps for  $C_2H_3CN$ ,  $C_2H_5CN$ ,  $HC_3N$ , and  $CH_3CN$ . The coordinate scale is in Titan-projected distances. Titan's surface (blue circle) and polar axis (dot-dashed line) are marked. Contour intervals (in units of  $\sigma$  — the RMS noise level of each map), are as follows:  $C_2H_3CN$ :  $1.5\sigma$ ,  $C_2H_5CN$ :  $3\sigma$ ,  $HC_3N$ :  $3\sigma$ ,  $CH_3CN$ :  $4\sigma$ . The FWHM of the Gaussian restoring beam ( $1.22'' \times 0.62''$ ) and its orientation is shown with hatched ellipses.

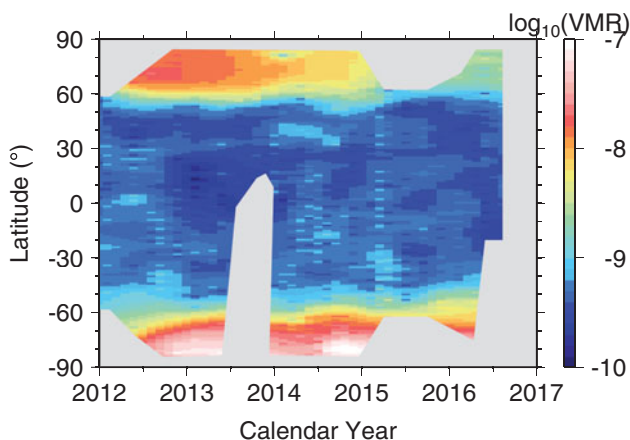
compare transitions that all originate from similar (ground-state) vibrational energy levels. Ideally, the exact same  $\Delta J$  transition should be observed across multiple epochs, but for the present study, we have to work within the limitations of the serendipitous  $HC_3N$  detections available in the ALMA Science Archive.

Figure 3 shows a time series of  $HC_3N$  observations from 2012-07-04 to 2015-08-29. These observations include the transitions  $J = 26 - 25$ ,  $40 - 39$  and  $35 - 34$  in the vibrational ground state, and are expected to probe similar regions of the atmosphere. The  $J = 26 - 25$  transition was observed on both the first and the final epoch, which helps rule out differences in thermal excitation as a cause for the observed variations. As explained by Lai *et al.* (2017), for the purpose of the present study, 5-10 K differences in temperature between Titan's north and south polar regions (as seen in Cassini  $CH_4$  temperature data) are expected to have negligible impact on the relative emission intensity from these lower-energy  $HC_3N$  transitions observed by ALMA.

The panels on the right of Figure 3 show the total  $HC_3N$  flux for each epoch, extracted along a line from south to north across Titan's disk. These 'latitudinal profiles' provide a clearer view of the temporal variation, and highlight the tendency for  $HC_3N$  to be strongly peaked around both poles. The relative strength of the southern peak increases year-on-year, consistent with the buildup of  $HC_3N$  at the winter pole as a result of transport from its main production site at mid-latitudes. Between 2014 to 2015, the



**Figure 3.** Titan  $\text{HC}_3\text{N}$  flux contour maps (left) and latitudinal profiles (right) for four epochs. Latitudinal profiles show the flux extracted along the polar axis from south to north (dashed line). Fluxes are normalized to the peak value ( $S_p$ ) and the contour intervals are in units of  $S_p/7$ . Vertical lines in right-hand panels indicate the positions of Titan's S and N (polar) limbs.



**Figure 4.** Cassini CIRS stratospheric  $\text{HC}_3\text{N}$  abundances as a function of latitude and time, using nadir observations of the vibronic emission band at  $663\text{ cm}^{-1}$  Teanby *et al.* (2017). Grey indicates missing data.

northern peak underwent a dramatic reduction in relative strength, indicative of a rapid loss of  $\text{HC}_3\text{N}$  around the north pole over a 17 month period.

#### 4. Discussion

The loss of photochemically-derived gases from the north and their buildup in the south since 2012 is consistent with the trend observed by Cassini in  $\text{HC}_3\text{N}$  and other short-lived molecules on Titan. A time series of  $\text{HC}_3\text{N}$  abundances is shown as a function of latitude in Figure 4. These data are based on observations using the Cassini Infrared Spectrometer (CIRS), following the method outlined by Teanby *et al.* (2010). This figure also confirms the degree to which  $\text{HC}_3\text{N}$  is confined about the poles. The steady trend for decreasing  $\text{HC}_3\text{N}$  abundances at the north pole ( $> 60^\circ$  latitude), with corresponding, rapid increase at the south pole ( $< -60^\circ$ ) since 2012 supports the reversal of Titan's global Hadley-type circulation cell within a few years after the 2009 equinox, as predicted by general circulation models (e.g. Newman *et al.* 2011; Lebonnois *et al.* 2012). The circulation cell occurs due to warm air rising over the summer hemisphere and sinking in the vicinity of the winter pole, and extends to altitudes above 500 km. This results in advection of gases (including the observed nitriles), from their source region in the upper atmosphere to the lower atmosphere, creating enrichment near the winter pole. When this circulation pattern reverses after equinox, the advective source term is removed and the enriched gases disperse and photochemically break down at a rate determined by their lifetime. The rapid (order of magnitude) loss of  $\text{HC}_3\text{N}$  at the north pole from 2012-2016 confirms the short chemical lifetime for this species.

The persistence of a northern-hemisphere enhancement for  $\text{CH}_3\text{CN}$  in 2015 (see Figure 2, bottom right), is indicative of a longer lifetime for this species in Titan's atmosphere, which agrees with prior theoretical expectations (e.g. Wilson & Atreya 2004; Krasnopolsky 2009). The more recent model of Loison *et al.* (2015) also found longer lifetimes for  $\text{CH}_3\text{CN}$  and  $\text{C}_2\text{H}_5\text{CN}$  than for  $\text{HC}_3\text{N}$  and  $\text{C}_2\text{H}_3\text{CN}$ . These differences in reactivity are related to molecular structure. For example,  $\text{CH}_3\text{CN}$  and  $\text{C}_2\text{H}_5\text{CN}$  are fully saturated, whereas  $\text{HC}_3\text{N}$  and  $\text{C}_2\text{H}_3\text{CN}$  are unsaturated. The saturated molecules are less likely to react with hydrogen-rich species in Titan's reducing atmosphere, which explains their longer lifetimes. Photolysis rates for  $\text{CH}_3\text{CN}$  and  $\text{C}_2\text{H}_5\text{CN}$  are also predicted to be lower



than for HC<sub>3</sub>N and C<sub>2</sub>H<sub>3</sub>CN as a result of UV line shielding by CH<sub>4</sub> (J. C. Loison 2017, private communication).

We find reasonable qualitative agreement between the photochemical lifetimes apparent from observations and those predicted by chemical models. This suggests that current theoretical understanding of Titan's complex nitrile chemistry is reasonably good. However, the chemistry of the observed nitriles is currently not fully constrained, which limits their use as probes of Titan's atmospheric dynamics. Additional laboratory experiments will be required to improve our knowledge of their chemical formation and loss pathways, which will be vital for a full understanding of the chemistry of these species in planetary atmospheres, as well as interstellar environments.

## 5. Conclusion

ALMA observations of Titan's atmospheric gases, including the first map of C<sub>2</sub>H<sub>3</sub>CN and a detailed time series of HC<sub>3</sub>N measurements, are consistent with rapid photochemical production, transport and loss of these molecules over periods of a few Earth years. The abundance patterns for the different nitriles are explained as a result of their individual photochemical lifetimes, combined with the latitudinally-dependent, seasonal variations in atmospheric temperature and radiation input that give rise to changes in the direction of Titan's high-altitude global circulation cell.

The ability to obtain hemispheric maps of short-lived nitriles confirms the important role for ALMA in continuing Cassini's legacy for detailed studies of Titan's climate and chemistry. Ongoing observational, laboratory and theoretical studies are required to improve our understanding of Titan's atmospheric chemistry and dynamics, with applications to primitive planetary atmospheres in our Solar System and beyond.

## Acknowledgements

This work was supported by The Goddard Center for Astrobiology, the National Science Foundation (under Grant No. AST-1616306) and the UK Science and Technology Facilities council. It makes use of ALMA data set ADS/JAO.ALMA#2013.1.00033.S. ALMA is a partnership of ESO, NSF (USA), NINS (Japan), NRC (Canada), and NSC and ASIAA (Taiwan), in cooperation with the Republic of Chile. The Joint ALMA Observatory is operated by ESO, AUI/NRAO, and NAOJ. The NRAO is a facility of the National Science Foundation operated under cooperative agreement by Associated Universities, Inc.

## References

- Bézard, B., Yelle, R., & Nixon, C. A. 2014, in Titan: Surface, Atmosphere and Magnetosphere, ed. I. Muller-Wodarg, C. Griffith, E. Lellouch, & T. Cravens (Cambridge, UK: Cambridge Univ. Press), 158
- Cordiner, M. A., Nixon, C. A., Teanby, N. A., *et al.* 2014, *ApL*, 795, L30
- Cordiner, M. A., Palmer, M. Y., Nixon, C. A., *et al.* 2015, *ApL*, 800, L14
- Cui, J., Yelle, R. V., Vuitton, V., *et al.* 2009, *Icarus*, 200, 581
- Hörs, S. M. 2017, *JGRE*, 122, 432
- Lai, J. C., Cordiner, M. A., Nixon, C. A. *et al.* 2017, *AJ*, submitted
- Lebonnois, S., Burgalat, J., Rannou, P., & Charnay, B., 2012, *Icarus*, 218, 707
- Loison, J. C., Hébrard, E., Dobrijevic, M., *et al.* 2015, *Icarus*, 247, 218
- Krasnopolsky, V. A. 2009, *Icarus*, 201, 226
- Newman, C. E., Lee, C., Lian, Y. *et al.* 2011, *Icarus*, 213, 63
- Palmer, M. Y., Cordiner, M. A., Nixon, C. A., *et al.* 2017, *Sci. Adv.*, 3, e1700022

- Stevenson, J., Lunine, J., & Clancy, P. 2015, *SciA*, 1, e1400067
- Teanby, N. A., Bezard, B., Vinatier, S. *et al.* 2017, *Nature Communications*, 8, 1586
- Teanby, N. A., Irwin, P. G. J., de Kok, R., & Nixon, C. A. 2010, *ApJ*, 724, L84
- Teanby, N. A., Irwin, P. G. J., Nixon, C. A., *et al.* 2012, *Natur*, 491, 732
- Teanby, N. A., Irwin, P. G. J., Nixon, C. A., *et al.* 2013, *P&SS*, 75, 136
- Vinatier, S., Bézard, B., Lebonnois, S., *et al.* 2015, *Icarus*, 250, 95
- Vuitton, V., Yelle, R. V., & McEwan, M. J. 2007, *Icarus*, 191, 722
- Wilson, E. H. & Atreya, S. K. 2004, *JGRE*, 109, 6002